Published in final edited form as:
Biochemistry. 2006 June 27; 45(25): 7693–7699.

Dynamic coupling and allosteric behavior in a non-allosteric protein†

Michael W. Clarkson‡, **Steven A. Gilmore**, **Marshall H. Edgell**‡,§, and **Andrew L. Lee**‡,*
University of North Carolina at Chapel Hill

‡*Department of Biochemistry and Biophysics, School of Medicine*

§*Department of Microbiology and Immunology, School of Medicine*

Abstract

Long-range intraprotein interactions give rise to many important protein behaviors. Understanding how energy is transduced through protein structures to either transmit a signal or elicit conformational changes is therefore a current challenge in structural biology. In an effort to understand such linkages, multiple V→A mutations were made in the small globular protein eglin c. The physical responses, as mapped by NMR spin relaxation, residual dipolar couplings (RDCs), and scalar couplings, illustrate that the interior of this non-allosteric protein forms a dynamic network and that local perturbations are transmitted as dynamic and structural changes to distal sites as far as 16 Å away. Two basic types of propagation responses were observed: contiguous pathways of enhanced (attenuated) dynamics with no change in structure; and dispersed (non-contiguous) changes in methyl rotation rates that appear to result from subtle deformation of backbone structure. In addition, energy transmission is found to be unidirectional. In one mutant, an allosteric conformational change of a side chain is seen in the context of a pathway of propagated changes in ps-ns dynamics. The observation of so many long-range interactions in a small, rigid system lends experimental weight to the idea that all well-folded proteins inherently possess allosteric features [Gunasekaran et al. (2004) *Proteins* 57, 433−443], and that dynamics are a rich source of information for mapping and gaining mechanistic insight into communication pathways in individual proteins.

Protein function is intimately tied to changes in the conformational ensemble (2). In classically allosteric proteins, perturbations such as ligand binding or chemical modification alter the conformation of distal sites, thereby modulating binding affinity or catalytic efficiency. Because this property is fundamental to regulation and signaling, the creation of allosteric systems will likely emerge as a challenge for the maturing fields of protein engineering and design. To that end, it is necessary to determine what features of real proteins give rise to coordinated long-range structural and energetic changes.

An intuitively satisfying model for long-range interactions is a stereochemical mechanism (3,4) wherein residue modification or ligand binding leads to a local conformational change that is mechanically propagated via residue-residue interactions to the active site. Consistent with this model is the identification of evolutionarily conserved sparse networks of

†This research was supported by NIH grant GM066009.

*Correspondence: Division of Medicinal Chemistry and Natural Products, School of Pharmacy, Beard Hall -CB#7360, Chapel Hill, NC 27599−7360 email: drewlee@unc.edu, phone: (919) 966−7821, fax: (919) 843−5150.

Supporting information
Changes in ^{15}N order parameters (S^2) are available for V13A, V18A, V34A, V62A, and V63A (Fig. 5). Changes in methyl S^2_{axis} parameters are available for V13A and V63A (Fig. 6). A complete analysis of the populations of χ_1 angles in valine and threonine residues are provided for WT, V18A, V34A, V54A, and V62A in Table 2. Tables 3-8 contain numerical S^2_{axis} and τ_e values, J-coupling constants, and ^{2}H relaxation rates at 500 and 600 MHz. This material is available free of charge via the Internet at http://pubs.acs.org.

communication within globular proteins (5). These studies develop a picture of protein interiors as highly interconnected, with combinations of residues that are "aware" of one another, even at long distances. This picture is consistent with numerous measurements of non-zero thermodynamic couplings (ΔG_i) (6) between non-contacting residues (7,8). A variety of computational approaches lend mechanistic insight into coupling networks (9-13), many of which implicate correlated motions as fundamental to long-range communication and conformational switches. Yet it remains a challenge to complement *in silico* studies with *in vitro* results.

Here, we take a perturbational approach to obtain experimental insight into the behavior of a communication network in the interior of a single, natively folded protein. We have taken advantage of the high valine content of eglin c, a homologue of chymotrypsin inhibitor 2 which has been used in numerous studies of folding and stablity (14), to dissect the dynamic network via a perturbation-response strategy. Mapping the dynamic response to perturbations should reveal specifics about the underlying forces present in the network, and, in the case of mutational perturbations, simulate evolutionary changes of coupling networks. Unlike many enzymes, eglin c has little evidence of motion on the μs-ms timescale, yet like all proteins, it possesses extensive side-chain motions on the ps-ns timescale (15,16). Dynamic responses to several valine-to-alanine mutations were analyzed using the model-free formalism (17), and analyzed for network behavior. The results indicate that the effects of even conservative site mutations can be transduced throughout the protein, in a manner indistinguishable from true allostery, even in cases where the backbone conformation is preserved. Although responses are highly context-dependent, two main *types* of responses were observed: contiguous (traceable pathway) and disperse (non-traceable). In addition, dynamic transduction between two network sites is not, in general, bidirectional, in agreement with theoretical prediction (18). Most mutations influence distal regions of the structure, and some are associated with energetic coupling, raising the possibility that native state dynamics may cause or signify some long-range thermodynamic couplings.

Experimental Procedures

Protein preparation and NMR data acquisition

Protein expression and purification were performed as described previously using eglin c with the same F10W background (19). NMR experiments were performed on 2 mM (V34A, V13A) or 1 mM (V18A, V62A, V63A) protein in a standard buffer (20 mM KH_2PO_4, 50 mM KCl, 0.02% NaN_3, pH 7.0) at 37 °C, with the exception of V63A, for which data were collected at 25 °C. Relaxation data for WT were previously collected at 2 mM and 37 °C (19); additional datasets at 1 mM were collected at 25 °C and 37 °C for comparison to the mutants above. Internal dynamics parameters for WT at 1 mM and 2 mM concentrations were found to be essentially identical, and therefore parameters from the WT 2 mM sample were used for comparisons to mutants. NMR data were acquired using gradient-equipped Varian INOVA spectrometers operating at 500 and 600 MHz. ^{15}N CPMG-based T_2 measurements were employed with relaxation delays of 8, 16, 24, 40, 63, 79, 95, 111, and 127 ms. Relaxation delays in T_1, $I_zC_zD_z$, $I_zC_zD_y$, and I_zC_z experiments were identical to those used in previous work on eglin c (19). Errors were assessed by analyzing duplicate timepoints (underlined in the preceding list). All spectra were processed using NMRPipe (20) and analyzed with the assistance of NMRView (21).

Relaxation Analysis

Order parameters for backbone and side-chain groups were calculated on the basis of the simple model-free formalism (17) using relxn2.1 (22) and the front-end interface relaxvi.

Chemical Denaturation

Chemical denaturation experiments were performed as previously described (19) using an Aviv autotitrating fluorometer. The $\Delta\Delta G_U$ values were calculated by subtracting the mutant from the wild-type, and $\Delta\Delta\Delta G_i$ values were calculated using:

$$\Delta\Delta\Delta G_i = \Delta G_{U,WT} + \Delta G_{U,AB} - \Delta G_{U,A} - \Delta G_{U,B}$$

where A and B represent the single mutants and AB represents the double mutant. A uniform error estimate was applied using a weighted average of the standard deviation of measurements for each mutant, yielding an average error of 0.09 kcal/mol, which is similar to errors observed in previous experiments on thermodynamic coupling (7,23).

Rotamer population analysis

Rotamer populations for valines and threonines were calculated from 3-bond J_{NC} and J_{CC} couplings measured using a quantitative *J*-correlation method (24,25). Once acquired, the couplings were then analyzed using a jump-diffusion model (26). Values of $^3J_{trans}$ and $^3J_{gauche}$ were adopted from previous work by Wright and coworkers (27). For valines, the results from the two individual methyl groups were averaged. In some cases (mostly threonines) the sum of the calculated populations was greater than one. Because these results are consistent across all mutants, it is probably due to deficiencies in the model.

RDC data analysis

Residual dipolar couplings were determined using nonionic lipid bicelles as an orienting medium (28) and IPAP experiments. Couplings were acquired once for each of a set of mutants (V13A, V14A, V34A, V54A, V62A, V63A) and twice for wild-type. Linear relationships were calculated for each mutant compared to WT, and the two WT results were fit to each other. Residuals from these fits were then collated for statistical analysis.

Results

In an effort to understand energy transmission in proteins, we have initiated a study to analyze the structural and dynamic responses to mutational perturbations in the globular protein eglin c. In total, seven of ten valines distributed within the globular region of eglin c were mutated to alanine, and these mutants were characterized by a variety of NMR measurements to assess the adaptation of the protein ensemble. The behavior of mutants V13A, V18A, V34A, V62A, and V63A are presented here; two other mutants (V14A, V54A) were reported previously (19). V13, V18, V34, V54, and V63 are fully buried in the core, whereas V14 and V62 are partially exposed to solvent. All of these valines are in the globular core domain (not the reactive loop) of eglin c.

V34A

Lipari-Szabo order parameters were determined for backbone NH (S^2) and side-chain C-CH_3 (S^2_{axis}) bond vectors using ^{15}N and ^2H relaxation, respectively. The backbone NH order parameters are slightly reduced in V34A relative to WT, with an average ΔS^2 of −0.02 (Supp. Info., Fig. 5). Nearly all residues show a slight increase in ps-ns flexibility, indicating a subtle global backbone effect. The ps-ns dynamics of the side chains, however, are more significantly perturbed (Fig. 1D, E). A threshold of twice the standard deviation was applied to differentiate significant and insignificant responses. Changes in both S^2_{axis} and τ_e values are positive and negative and are observed in a predominantly contiguous pathway that extends beyond the site of mutation (Fig. 2). For example, V18 is 11 Å from V34 (C^β-C^β distance), and both V18 methyl order parameters decrease by 0.10 (and τ_e increases by ~7 ps). Analysis of 3-bond J-coupling constants for N-C^γ and C'-C^γ indicate that the χ_1 = 180° rotamer population in V18

and V52 shifts from 86% and 81% to 68% and 47%, respectively (Supp. Info., Table 2). Perhaps even more striking is that the τ_e value of the V62 γ2 methyl decreases from 39.3 ± 1.4 ps to 34.8 ± 0.8 ps even though it is 16 Å from V34.

To assess changes to the time-averaged structure, backbone ^1H-^{15}N residual dipolar couplings (RDCs) were measured for both WT and V34A. The RDCs of V34A are identical to WT (within the reproducibility of these measurements) with $r^2 = 0.99$ (Fig. 1F), and we conclude that the backbone structure of V34A is unperturbed.

V18A and V62A

For V18A and V62A mutants, changes in ps-ns backbone dynamics are generally too small to be significant and reliable (Supp. Info., Fig. 5). In V18A, the changes to S^2_{axis} are nearly non-existent (Fig. 1A), but a number of significant changes in side-chain τ_e values are apparent (Fig. 1B), with V52 and V62 showing wildly different methyl τ_e values compared to WT. We interpret this as a major change in the rapid 3-fold rotation rate of these four methyl groups (22). Interestingly, V52 is 13 Å away (C^β-C^β) from the site of mutation (based on pdb entry 1CSE) – two shells of neighboring residues removed. V62 is also not in contact with V18A, at a distance of 7.3 Å. RDC measurements of V18A show a strong correlation relative to WT (Fig. 1C), consistent with an unchanged overall structure of the mutant. However, the correlation is somewhat weaker than in the case of V34A (or V54A), with $r^2 = 0.96$, indicating some subtle structural deformation in V18A.

V62A shows similar features to V18A, although the changes are subtle (Figure 1G, H). The ps-ns backbone dynamics are unperturbed, as are the side-chain S^2_{axis} values. However, there are small but significant changes in the side-chain τ_e values which, like V18A, are accompanied by subtle changes in RDC values (Fig. 1I, $r^2 = 0.97$). This highlights the sensitivity of using methyl τ_e values as a probe for change in local environment.

V63A and V13A

V63A, though destabilized by 3.2 kcal/mole (Table 1) and in the middle of a dynamic network (see Discussion, Fig. 2), exhibits only a few local changes in backbone and side-chain dynamics (Supp. Info., Figs. 5-6). As assessed from relaxation measurements, RDCs, and chemical shifts, the structure and dynamics of this mutant appear to be unchanged (except for residues neighboring A63). Similar observations were made for V13A eglin c, although for this mutant small, uniform changes in S^2_{axis} and τ_e were observed, which may be due to a systematic error in the relaxation data due to non-specific aggregation or other source of bias. In summary, V63 and V13A perturbations, despite their location in the core of the protein, do not appear to cause propagated changes in structure or dynamics.

Double-mutant cycles

Double-mutant cycles were constructed involving V18, V34, V54 and V62, and coupling free energies were determined with respect to protein unfolding (Table 1). Four couplings are small but fall outside of the determined error, and one coupling (V18A,V54A) is substantial at −0.95 kcal/mole, even though V18 and V54 are not in contact and the closest side-chain carbon atoms are 6.6 Å apart.

Discussion

To gain insight into the nature of communication networks in proteins, we have observed the behavior of the network in a single protein. The majority of valines in eglin c have been mutated to alanine and the physical effects monitored in solution at atomic resolution using NMR spectroscopy. Each of the seven “responses” are different, but most striking is that a single site

mutation can reverberate throughout most of the structure (Figs. 2-3). Essentially all dynamic responses are on the ps-ns timescale. ^{15}N T_2 experiments show little sign of significant μs-ms motion in any of the mutants studied, although line-broadening in spectra were consistently observed for several residues in the reactive site loop and V66. Relaxation dispersion ^{15}N CPMG experiments (29) were carried out on WT, V14A, V18A, and V62A mutants (data not shown); essentially no motions on the μs-ms timescale were detected with these experiments. Side-chain responses on the ps-ns timescale, however, reveal two distinct behaviors.

Two kinds of dynamic responses

"contiguous" and "disperse". For the five mutants that show long-range propagation of dynamic changes, two main types of dynamic responses are observed. The V34A mutation alters dynamics primarily in a contiguous path of residues (Fig. 2), in a manner reminiscent of V14A and V54A (19). In addition, from ^{1}H-^{15}N RDCs, the backbone structures of all three of these mutants appear to be identical to WT. Therefore, the responses appear to be purely dynamic in nature. This "contiguous network response" appeals to intuition and directly supports the notion of dynamic communication pathways. By contrast, V18A and V62A show dynamic response patterns in which side chains that have altered motional parameters are scattered throughout the structure (Fig. 3). These two "disperse network responses" are marked by 1) responding residues that are not in van der Waals contact with one another, 2) a predominance of τ_e changes (with minimal S^2_{axis} changes), and 3) subtle structural effects (see below) that coincide with some of the sites with altered dynamics. These two mutants illustrate that a simple mutation can have a marked effect at distal sites even in the absence of a clear pathway. While all mutants showing propagated dynamic changes appear to fall into either of these response types, one can imagine other mutants showing features of both.

On a technical note, it should be mentioned that because side-chain motions may occur at more than one timescale, use of a simple internal order parameter (S^2_{axis}) and characteristic time (τ_e) may not reflect pure motional amplitudes in some side chains. Motions on the timescale of a few nanoseconds have been detected using an expanded suite of five ^{2}H side-chain relaxation experiments in concert with the "LS-3" model (30). Attempts to use the LS-3 model with the present ^{2}H relaxation data resulted in unstable fits or parameters with unacceptably high uncertainties, underscoring the need for the additional three experiments when using this model. Collection of additional ^{2}H relaxation data was not carried out since the primary goal was simply to observe *changes* in dynamics. This is most simply done by comparison of equivalent model-free parameters. Use of additional ^{2}H relaxation rates will be useful for future characterization.

Allostery and bidirectional transmission in the network

One of the most striking results is that allosteric-like signaling is found in eglin c. Upon V34A mutation, a discrete conformational change takes place 11 Å from the site of mutation in the side chain of V18, which is buried in the WT structure. As determined from 3-bond N-C^{γ} and C'-C^{γ} coupling constants, the V18 χ_1 rotamer distribution goes from 0.14/0.01/0.86 (−60°/60°/180°) in WT to 0.11/0.21/0.68 in V34A (Table 2). This increased rotamer sampling is consistent with a decrease in S^2_{axis} from 0.5 to 0.4, which suggests that approximately half of this population change is due to increased χ_1 rotamer switching on the timescale of picoseconds to ~10 ns (31); the other half must be due to slower switching on timescales between ~10 ns and a few milliseconds. This side-chain conformational change is in direct response to mutation at V34 and occurs in the context of a contiguous network response and an unaltered (backbone) structure. Although double-mutant cycle analysis does not find a free-energy coupling congruent with this propagated conformational change (ΔG_i = −0.02 kcal/mole, Table 1), this may only reflect that the linkage does not impact on the protein's stability. The conformational change resulting from dynamic transmission and our repeated observations of long-range

propagation support the idea that all globular proteins harbor intrinsic allosteric behavior (1). Most significant is that such behavior is found in a monomeric, unregulated, non-enzymatic, and ostensibly rigid protein that has no known functional allostery.

If a V→A mutation can signal from site 34 to 18, will the reverse be true? In this particular case, the answer is clearly "no" (Fig. 1A,B), and this appears to be the general trend. In WT eglin c, the V18 and V54 side chains oppose one another with closest carbon atoms 7 Å apart. The V54A mutation induces a substantial increase in S^2_{axis} at V18 (increase of 0.17 ± 0.02) (19), which is the largest dynamic change in all of the mutants studied to date. For the reverse perturbation, the V18A mutation has no effect on either S^2_{axis} or τ_e of V54 (Fig. 1A,B). Similarly, the V54A mutation alters the dynamics of V62 (19), over 11 Å away, but the V62A mutation does not signal back to V54 (Figure 1G, H). Some excitory pathways in eglin c do appear to have some degree of bidirectionality, however. One example is V34A/V62A, in which V34A leads to a decrease in V62 τ_e and V62A leads to a τ_e change at V34. The response in V62A is disperse in nature, and so even though the propagation from V34A appears to travel by a "path", the reverse response does not. Based on these observations, energy transmission is often not bidirectional. This confirms the remarkable prediction put forth by Hilser, Freire, and colleagues using simulated conformational ensembles, although in that case "local unfolding" was probed rather than ps-ns side-chain fluctuations (18). In the evolution of protein sequences, a lack of bidirectionality may allow for certain regions of the protein (such as the active site) to be under greater control than other regions.

Because V63 appears to be a central residue in the protein core (and network), it is interesting (perhaps surprising) that V63A exhibits minimal dynamic and structural responses. V63 is inferred to participate in dynamic propagation in all of the contiguous network responses (19). Because of its centrality and importance for stability (Table 1), it is tempting to think of V63 as a network hub. Unfortunately, the dynamics of V63 are rarely apparent due to spectral overlap in most of the mutants, although when observable, the side-chain of V63 appears to be rigid ($S^2_{axis} \approx 0.8$). As mentioned by others, rigid residues may be efficient transducers of motion or energy (32).

Structural component to "disperse" responses

Comparisons of WT RDCs with those of the two mutants that exhibit disperse network responses (V18A, V62A) produce correlation coefficients < 0.98, the lowest seen among the V→A mutants. Residuals from linear fits (vs. WT RDCs) from eight variants were determined to yield a standard deviation of 1.91 Hz. A cutoff of twice this value was used to identify the most significant RDC outliers. In V18A, 6 outliers were identified, four of which (residues 50, 51, 54, 55) cluster within β-strand 2 (Fig. 3A, 4A). As the magnitude of these four RDC values are all reduced relative to WT, β2 appears to undergo an untwisting motion, leaving the orientation of the central residue NH bond vectors (RDCs near 0 Hz) unchanged while the NH bonds of the outer residues rotate in opposite directions (RDCs attenuated). A shift within this strand is supported by an anomalously reduced backbone order parameter in V18A at H65 (Fig. 5), which in WT forms a hydrogen bond with F55, suggesting a breaking of this bond. In addition, significant chemical shift changes relative to WT were observed for Y56 (in contact with V18) and N57. The RDC residuals in V18A reflect a structural change either 1) as a movement of the average structural coordinates with little change in motional fluctuation about the average structure (i.e. a "static" structural change), or 2) as a large amplitude dynamic motion of β2 that fluctuates about or from the WT coordinates on a sub-millisecond timescale.

In the case of V62A, five residues qualify as outliers (Fig. 4B), several of which cluster in a banded pattern at the N-termini of β1 and β2 (Fig. 3C). Unlike V18A, these RDC's both increase and decrease relative to WT, making the structural origin less obvious. Nevertheless, the clustering of RDC outliers in both V18A and V62A is suggestive of concerted structural

readjustment within the β-sheet. Also important here is that in V18 and V62, no significant changes in side-chain rotamers were detected from *J*-coupling constant analysis (Supp Info. Table 2). We conclude that subtle backbone adjustments are likely responsible for the changes in methyl rotation rates at disconnected sites that comprise the "disperse network responses" to mutation.

Distal energetic coupling correlates with largest change in dynamics

A hypothesis we wanted to test is whether dynamic couplings correlate with long-range thermodynamic couplings. Such a correlation would suggest that dynamic coupling information could be useful for the engineering of allosteric properties. The six free energy couplings measured to date in eglin c indicate a range of values, from −0.02 to −0.95 kcal/mole (Table 1). While the majority of values are small, most are slightly above error. Taken individually or in small numbers, these values would be considered insignificant, but collectively they appear to indicate non-zero coupling (8). In the case of V18A/V54A, the free energy coupling is sizeable at −0.95 kcal/mole. Unidirectional dynamic coupling was observed in V54A from V54→V18, yielding ΔS^2_{axis} of 0.17 ± 0.02 at both V18 methyls (19) and is in fact the largest long-range ΔS^2_{axis} in all eglin c mutants studied. This would appear to confirm, at least partially, the ability of dynamic couplings to predict thermodynamic couplings, although the structural changes in V18A prompt a caveat. In the RDC correlation plot for V18A vs. WT, V54 is an outlier (Fig. 4), which may reflect a change in structural environment at V54, which upon mutation to alanine (in the double mutant) could lead to a larger destabilization than in the absence of V18A. Another possibility is that the double mutant undergoes further structural change. These issues, due to the subtlety of the effect, may be difficult to parse. Conversely, the rigidification of the environment at V18 in V54A may contribute significantly to the additional destabilization upon V18A mutation relative to a wild-type background. In spite of these conjectures, it remains true that the largest observed dynamic coupling correlates with an unambiguous long-range thermodynamic coupling.

Conclusions

The small globular protein eglin c does not possess any obvious allosteric activity and functions primarily by providing a rigid body that prevents release from a target protease. Nonetheless, even in a protein of such limited size and function, fairly conservative mutations can alter dynamics at side chains more than 10 Å distant, through several layers of intervening residues. Energy transmission, however, does not appear to be bidirectional, as probed by multiple V→A mutations. The responses in NMR order parameters (S^2_{axis}) can be accompanied by subtle structural shifts (as in the case of V18A), altered rotamer populations (V18 and V52 in V34A), and energetic coupling. The knowledge that such perturbations tend not to be restrained to the immediate vicinity provides a reasonable basis for interpreting long-range thermodynamic coupling as a native state effect. Collectively, these results lend support to the idea that all folded proteins are allosteric entities (1). Additionally, the fact that dynamics measurements can reflect all these forms of communication indicates that even if the dynamics themselves are not the physical underpinning of the interactions, they will serve as an efficient means by which they may be identified. Knowledge of pre-existing communication pathways and allosteric properties in a given protein should prove to be critical information for guiding the engineering and design of new protein activities.

Acknowledgements

The authors would like to thank Karl Koshlap (UNC School of Pharmacy NMR Facility) and Greg Young (UNC Biomolecular Laboratory) for their technical assistance, Joshua Boyer for assistance in plasmid construction, and Jan Hermans for stimulating discussion.

Abbreviations

NMR, nuclear magnetic resonance; RDC, residual dipolar couplings; S^2, order parameter (ps-ns rigidity on a scale of 0−1) for N-H bond vector; S^2_{axis}, order parameter for C-CH_3 bond vector; τ_e, characteristic time for rapid methyl rotation; ΔG_i, free energy coupling.

References

1. Gunasekaran K, Ma B, Nussinov R. Is allostery an intrinsic property of all dynamic proteins? Proteins 2004;57:433–443. [PubMed: 15382234]
2. Kern D, Zuiderweg ERP. The role of dynamics in allosteric regulation. Curr. Opin. Struct. Biol 2003;13:748–757. [PubMed: 14675554]
3. Perutz MF. Stereochemistry of cooperative effects in haemoglobin. Nature 1970;228:726–734. [PubMed: 5528785]
4. Formaneck MS, Ma L, Cui Q. Reconciling the “old” and “new” views of protein allostery: A molecular simulation study of chemotaxis Y protein (CheY). Proteins. 2006published online 7 Feb 2006
5. Lockless SW, Ranganathan R. Evolutionarily conserved pathways of energetic connectivity in protein families. Science 1999;286:295–299. [PubMed: 10514373]
6. Horovitz A, Fersht AR. Strategy for analysing the co-operativity of intramolecular interactions in peptides and proteins. J. Mol. Biol 1990;214:597–629. [PubMed: 1696320]
7. Green SM, Shortle D. Patterns of Nonadditivity between Pairs of Stability Mutations in Staphylococcal Nuclease. Biochemistry 1993;32:10131–10139. [PubMed: 8399139]
8. LiCata VJ, Ackers GK. Long-range, small magnitude nonadditivity of mutational effects in proteins. Biochemistry 1995;34:3133–3139. [PubMed: 7880807]
9. Ichiye T, Karplus M. Collective motions in proteins: a covariance analysis of atomic fluctuations in molecular dynamics and normal mode simulations. Proteins 1991;11:205–217. [PubMed: 1749773]
10. Radkiewicz JL, Brooks CL. Protein dynamics in enzymatic catalysis: Exploration of dihydrofolate reductase. J. Am. Chem. Soc 2000;122:225–231.
11. Bahar I, Rader AJ. Coarse-grained normal mode analysis in structural biology. Curr. Opin. Struct. Biol 2005;15:586–592. [PubMed: 16143512]
12. Fetrow JS, Knutson ST, Edgell MH. Mutations of alpha-helical solvent-exposed sites of eglin c have long-range effects: Evidence from molecular dynamics simulations. Proteins 2006;63:356–372. [PubMed: 16342264]
13. Liu T, Whitten ST, Hilser VJ. Ensemble-based signatures of energy propagation in proteins: A new view of an old phenomenon. Proteins 2006;62:728–738. [PubMed: 16284972]
14. Fersht AR, Daggett V. Protein folding and unfolding at atomic resolution. Cell 2002;108:573–582. [PubMed: 11909527]
15. Wand AJ. Dynamic activation of protein function: a view emerging from NMR spectroscopy. Nat. Struct. Biol 2001;8:926–931. [PubMed: 11685236]
16. Hu H, Clarkson MW, Hermans J, Lee AL. Increased rigidity of eglin c at acidic pH: Evidence from NMR spin relaxation and MD simulations. Biochemistry 2003;42:13856–13868. [PubMed: 14636053]
17. Lipari G, Szabo A. Model-Free Approach to the Interpretation of Nuclear Magnetic Resonance Relaxation in Macromolecules: 1. Theory and Range of Validity. J. Am. Chem. Soc 1982;104:4546–4559.
18. Hilser VJ, Dowdy D, Oas TG, Freire E. The structural distribution of cooperative interactions in proteins: Analysis of the native state ensemble. Proc. Natl. Acad. Sci 1998;95:9903–9908. [PubMed: 9707573]
19. Clarkson MW, Lee AL. Long-range dynamic effects of point mutations propagate through side chains in the serine protease inhibitor eglin c. Biochemistry 2004;43:12448–12458. [PubMed: 15449934]
20. Delaglio F, Grzesiek S, Vuister GW, Zhu G, Pfeifer J, Bax A. NMRPipe - a multidimensional spectral processing system based on unix pipes. J. Biomol. NMR 1995;6:277–293. [PubMed: 8520220]

21. Johnson BA, Blevins RA. NMRView: A computer program for the visualization and analysis of NMR data. J. Biomol. NMR 1994;4:603–614.
22. Lee AL, Flynn PF, Wand AJ. Comparison of ^{2}H and ^{13}C NMR relaxation techniques for the study of protein methyl group dynamics in solution. J. Am. Chem. Soc 1999;121:2891–2902.
23. Chen J, Stites WE. Energetics of side chain packing in staphylococcal nuclease assessed by systematic double mutant cycles. Biochemistry 2001;40:14004–14011. [PubMed: 11705392]
24. Grzesiek S, Vuister GW, Bax A. A simple and sensitive experiment for measurement of Jcc couplings between backbone carbonyl and methyl carbons in isotopically enriched proteins. J. Biomol. NMR 1993;3:487–493. [PubMed: 8400833]
25. Vuister GW, Wang AC, Bax A. Measurement of three-bond nitrogen-carbon J-couplings in proteins uniformly enriched in 15N and 13C. J. Am. Chem. Soc 1993;115:5334–5335.
26. Hennig M, Bermel W, Spencer A, Dobson CM, Smith LJ, Schwalbe H. Side-chain conformations in an unfolded protein: chi-1 distributions in denatured hen lysozyme determined by heteronuclear 13C, 15N NMR spectroscopy. J. Mol. Biol 1999;288:705–723. [PubMed: 10329174]
27. Schnell JR, Dyson HJ, Wright PE. Effect of cofactor binding and loop conformation on side chain methyl dynamics in dihydrofolate reductase. Biochemistry 2004;43:374–383. [PubMed: 14717591]
28. Ruckert M, Otting G. Alignment of biological macromolecules in novel nonionic liquid crystalline media for NMR experiments. J. Am. Chem. Soc 2000;122:7793–7797.
29. Loria JP, Rance M, Palmer AG. A relaxation-compensated Carr-Purcell-Meiboom-Gill sequence for characterizing chemical exchange by NMR spectroscopy. J. Am. Chem. Soc 1999;121:2331–2332.
30. Skrynnikov NR, Millet O, Kay LE. Deuterium spin probes of side-chain dynamics in proteins. 2. Spectral density mapping and identification of nanosecond time-scale side-chain motions. J. Am. Chem. Soc 2002;124:6449–6460. [PubMed: 12033876]
31. Hu H, Hermans J, Lee AL. Relating side-chain mobility in proteins to rotameric transitions: Insights from molecular dynamics simulations and NMR. J. Biomol. NMR 2005;32:151–162. [PubMed: 16034666]
32. Ota N, Agard DA. Intramolecular signaling pathways revealed by modeling anisotropic thermal diffusion. J. Mol. Biol 2005;351:345–354. [PubMed: 16005893]
33. Koradi R, Billeter M, Wuthrich K. MOLMOL: a program for display and analysis of macromolecular structures. J. Mol. Graph. 1996

Supplementary Material

Refer to Web version on PubMed Central for supplementary material.

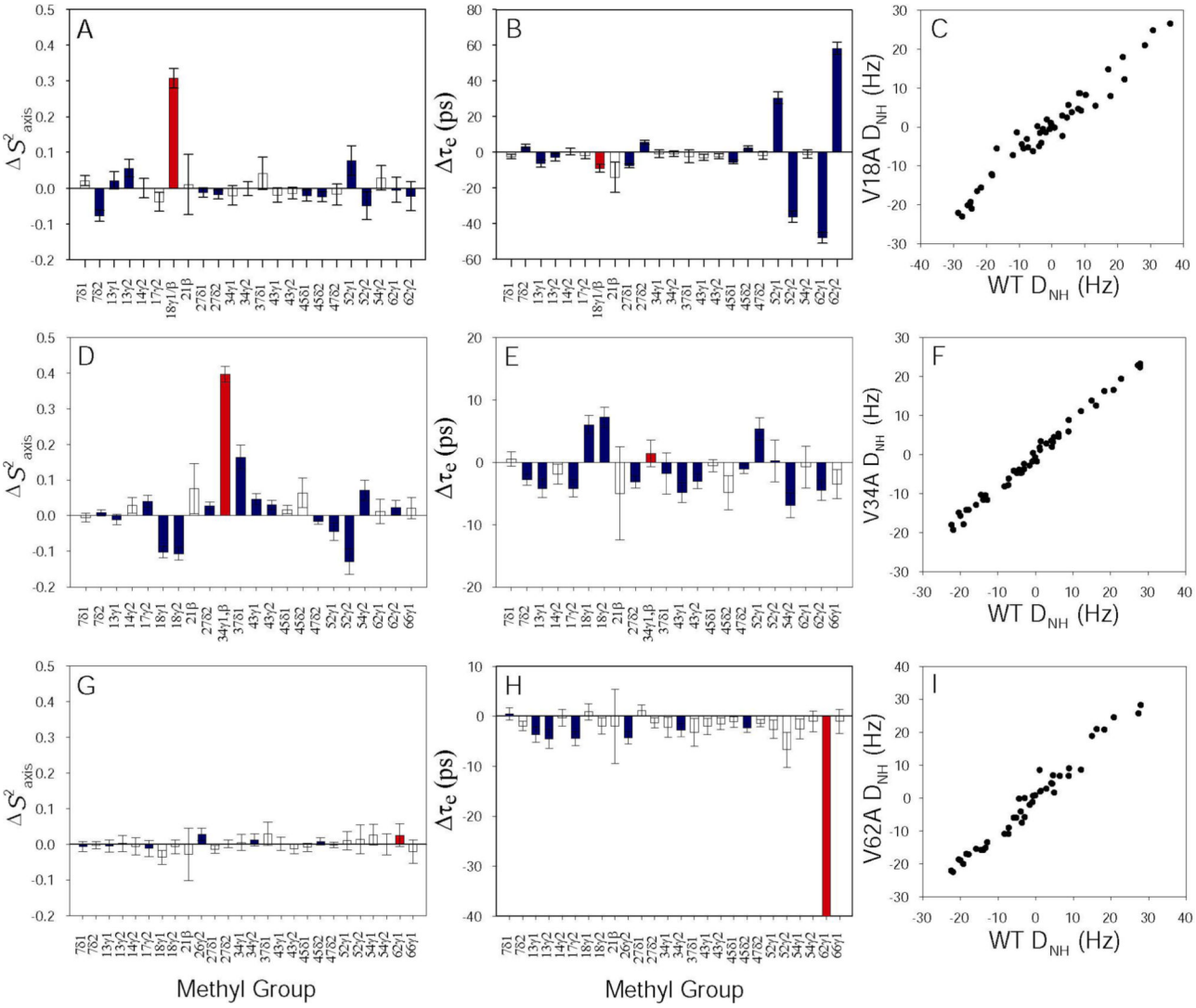

Figure 1.

Effects on side-chain S^2_{axis} (A, D, G), τ_e (B, E, H), and amide RDCs (C, F, I) of mutations V18A (A, B, C), V34A (D, E, F), and V62A (G, H, I). Bar graphs show changes in S^2_{axis} and τ_e (mutant – WT). Blue bars indicate changes in either S^2_{axis} or τ_e that were greater than twice the fitted error. Red bars indicate mutation sites, for which the new alanine is compared to the old γ_1 methyl group. Correlation coefficients (r^2) in panels C, F, and I are 0.96, 0.99, and 0.97.

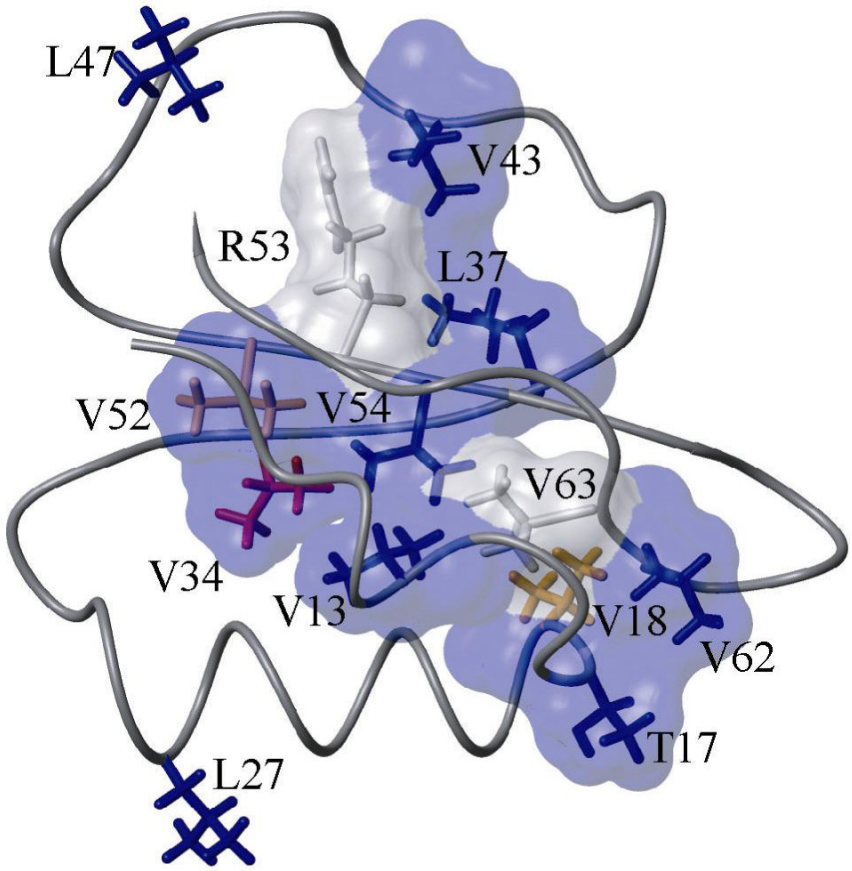

Figure 2.
Structure of WT eglin c (1CSE) showing side chains of residues participating in the "contiguous" dynamic network associated with the V34A mutation. Red sticks represent the mutated residue, orange sticks represent residues with clear changes in rotamer populations, and blue sticks represent residues which have clear changes in model-free parameters but do not in rotamer populations. Grey sticks represent residues which are included in the network because they form a bridge between clusters of responses, but for which no dynamics data are available. The contiguous surface was rendered as a contact surface using MOLMOL (33).

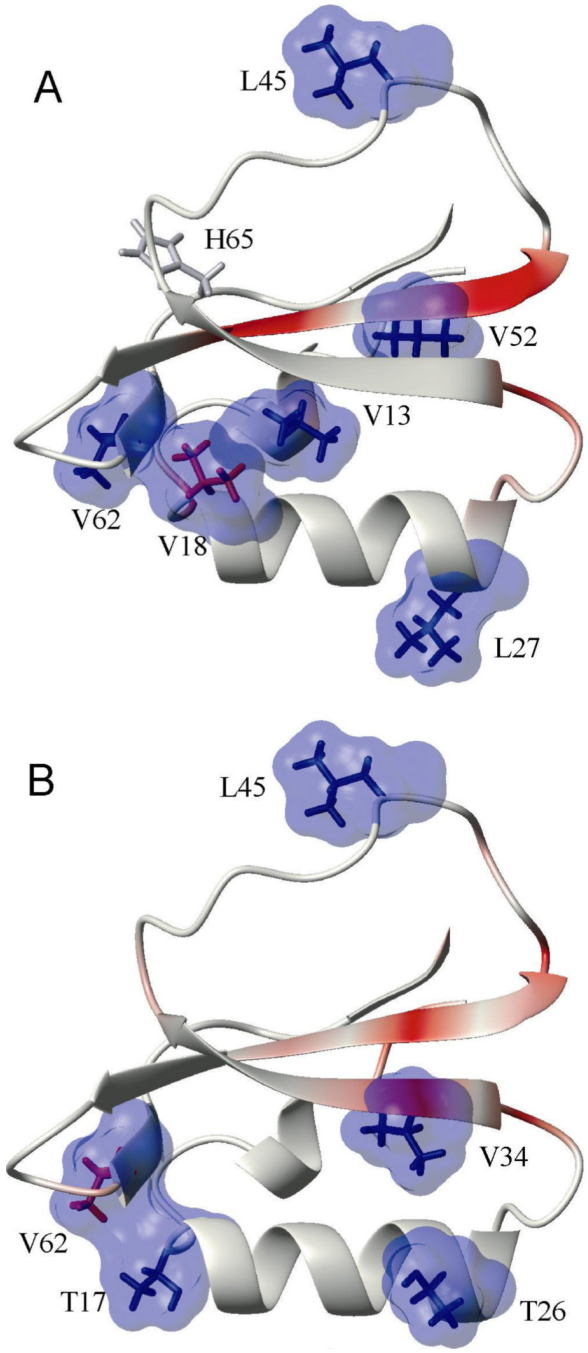

Figure 3.

Structures of WT eglin c showing residues participating in the “disperse” dynamic networks associated with V18A (A) and V62A (B) mutations. Orientations are rotated 180° about the z-axis relative to Figure 2, such that the long helix (containing V18) now appears in the foreground and V13 is in the background. Ribbons are colored red at residues that have amide RDCs over the 3.82 Hz threshold (see text) and pink at residues with residuals that are near but not over this limit. The side chain of the mutated residue is shown in red sticks, and those of residues with significant side-chain dynamic responses are shown in blue sticks. The side chain of H65 is depicted in grey sticks for the V18A mutant. Surfaces (rendered using the same method as in Figure 2) are shown for residues with side-chain dynamics responses; note that

V18 does not contact V62 or V13 in the WT structure (C^{β}-C^{β} distances of 7.3 and 10.0 Å, respectively).

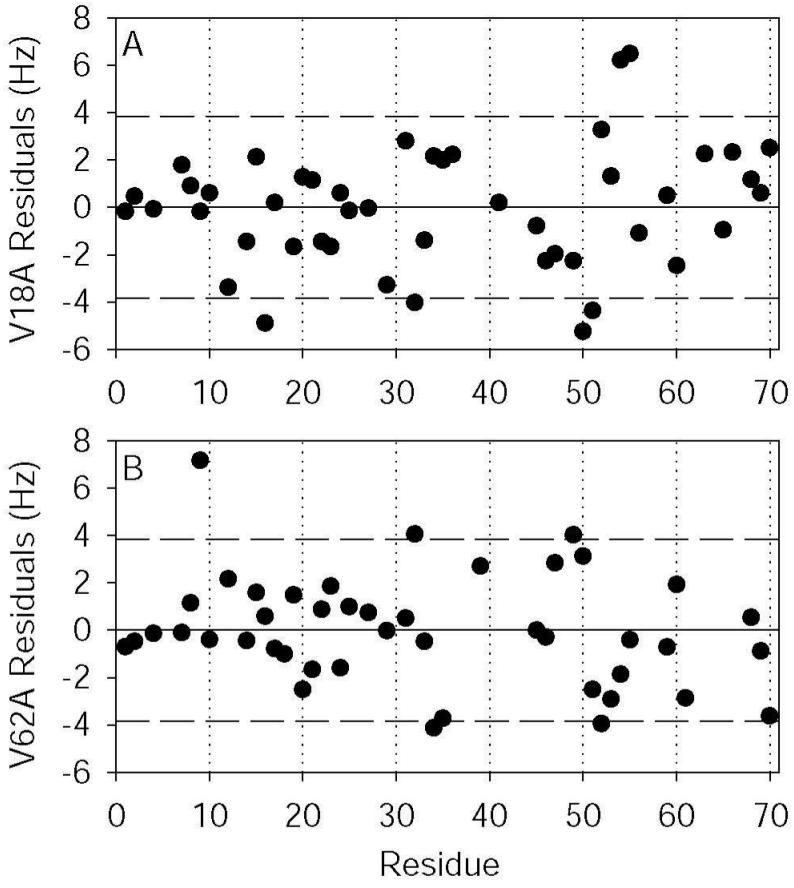

Figure 4.
Residuals associated with linear fits of V18A (A) and V62A (B) amide NH RDCs to corresponding WT RDCs. Dashed lines represent the ±3.82 Hz cutoff derived from the standard deviation of the residuals across 8 linear comparisons (see text).

Table 1

Energetics of unfolding for eglin c mutants. All values are in kcal/mol. Standard errors in $\Delta\Delta G_u$ and ΔG_i are 0.13 kcal/mole and 0.19 kcal/mole, respectively.

Mutant	$\Delta\Delta G_u$	ΔG_i
V18A[a]	−1.21	--
V34A	−1.27	--
V54A[a]	−1.59	--
V62A[a]	−1.02	--
V63A	−3.20	--
V14A/V18A[a]	−2.53	−0.27
L27A/V54A[a]	−1.98	−0.22
V54A/V62A[a]	−2.54	−0.26
V18A/V34A	−2.50	−0.02
V18A/V54A	−3.74	−0.95
V34A/V62A	−2.54	−0.25

[a] Values are updated from the originally determined values (19).